Available online at www.sciencedirect.com

ScienceDirect

IFAC Papers Online CONFERENCE PAPER ARCHIVE

IFAC PapersOnLine 50-1 (2017) 7699–7704

Bounded-voltage Power Flow Control for Grid-tied PV Systems

Yeqin Wang * **Beibei Ren** ** **Qing-Chang Zhong** ***

* *National Wind Institute, Texas Tech University, Lubbock, TX 79409, USA (e-mail: yeqin.wang@ttu.edu)*

** *Department of Mechanical Engineering, Texas Tech University, Lubbock, TX 79409, USA (e-mail: beibei.ren@ttu.edu)*

*** *Department of Electrical and Computer Engineering, Illinois Institute of Technology, Chicago, IL 60616, USA (e-mail: zhongqc@ieee.org)*

Abstract: An uncertainty and disturbance estimator (UDE)-based robust power flow control for grid-tied DC/AC converters was reported in the literature to achieve accurate power delivery in the presence of various types of model uncertainties and external disturbances. In this paper, a bounded-voltage power flow control is proposed for grid-tied PV systems with the improvement of the existing UDE-based robust power flow control to provide AC voltage protection. With the bounded-voltage design, the output voltage of the DC/AC converter always stays within the given range, which avoids the integrator windup caused by the saturation unit with the inappropriate setting of reactive power reference. Both simulation and experimental results are provided to demonstrate the effectiveness the proposed strategies.

Keywords: Grid-tied PV systems, Bounded-voltage power flow control, AC voltage protection, Integrator windup.

1. INTRODUCTION

Solar energy plays a very important role in energy industry, because replacing fossil-fuel combustion with solar energy reduces greenhouse gas emissions and air pollutions; sunlight is a free resource; and solar manufacturing costs and sales prices have dropped dramatically over the past few decades. One of the promising solar energy technologies, photovoltaic (PV), can directly convert sunlight into electricity based on one or two layers of semi-conducting materials. According to REN21's "Renewables 2016 Global Status Report", by the year of 2016, 7.3 gigawatts (GW) solar PV was installed in US, with a total of 25.6 GW of PV installation. While in Europe, about 7.5 GW of PV installation was added in 2016, bringing the region's total to almost 95 GW of operating solar PV capacity.

Since the sunlight resource is not controllable, and the output power of a PV source depends on the load conditions, power electronic converters are essential for converting the DC power generated by PV source into grid AC power with maximum power point tracking (MPPT) strategies, see Zhong and Hornik (2013). In some previous works, e.g. in Hua et al. (1998); Koutroulis et al. (2001); Killi and Samanta (2015), the PV source is often used for battery charging or other DC applications. With the growing of solar industry and energy requirement, the grid integration of PV source becomes very popular, e.g. in Femia et al. (2005); Deo et al. (2015); Montoya et al. (2016); Liu et al. (2015). In addition, most research on grid-tied PV system is focused on increasing the efficiency of the whole power system and the design of MPPT algorithms. An improved P&O MPPT algorithm is proposed in Femia et al. (2005). The distributed MPPT is discussed in Femia et al. (2008). Voltage-sensor-based MPPT with adaptive step size is addressed and analyzed in Killi and Samanta (2015). A modified incremental conductance algorithm that is able to track the global maximum power point under partial shading conditions and load variation is studied in Tey and Mekhilef (2014). A parameter-estimation-based MPPT is proposed in Teng et al. (2016). Other works focus on the topology of multiple-PV-source systems. A new topology of non-isolated per-panel DC/DC converters is studied in Walker and Sernia (2004). An intelligent modular system with optimal system performance is reported in Roman et al. (2006).

A typical topology of grid-tied PV systems has two power processing stages, including a DC/DC converter and a DC/AC converter, see Zhong and Hornik (2013). The DC/DC converter, usually a boost converter, converts the variable DC voltage power of the PV source into a constant DC voltage bus, see Femia et al. (2008); Pilawa-Podgurski and Perreault (2013); Deo et al. (2015); Montoya et al. (2016). Then DC/AC converter converts the constant DC voltage power into AC electrical grid. In some cases, multiply PV sources along with DC/DC converters share a common DC bus to simplify the system design. For the control of two-stage processing in grid-tied PV systems, the MPPT function is usually embedded into the DC/DC converter control. The DC-bus voltage is regulated by the DC/AC converter in most literature, e.g., in Femia et al. (2005); Deo et al. (2015); Montoya et al. (2016); Liu et al. (2015). And the proportional-integral (PI) controller is usually adopted for DC-bus voltage regulation to generate a current reference or a voltage reference, then the current controller or voltage controller is adopted for DC/AC converter with AC grid integration, see Femia et al. (2005); Deo et al. (2015); Montoya et al. (2016); Liu et al. (2015). Some other methods also can be used for grid-integration of DC/AC inverters, e.g., the vector control in Prodanovic and Green (2003); Trinh and Lee (2014), droop control methods in Kim et al. (2011); Nejabatkhah and Li (2015); Zhong et al. (2017), and virtual synchronous machines

2405-8963
Peer review under responsibility of International Federation of Automatic Control.
10.1016/j.ifacol.2017.08.1145

(VSM)-based control in Beck and Hesse (2007); Zhong and Weiss (2009, 2011); Zhong (2016). Recently, an uncertainty and disturbance estimator (UDE)-based robust power flow control is developed for DC/AC converters to achieve accurate power delivery to the grid in Wang et al. (2016a,b). It can achieve accurate regulation of both real power and reactive power, in the presence of model uncertainties (e.g., output impedance, power angle), the coupling effects, and the external disturbances (e.g., the fluctuation of DC-link voltage, variations of output impedance or line impedance, and variations of the grid voltage). Also, it does not require an extra synchronization unit in grid-connected operation.

An important issue for grid-tied PV systems is keeping the output voltage of inverters within the given range, particularity in the operation of islanded-mode microgrid or smart grid, see Zhong et al. (2016). Usually, the saturation units are applied to maintain the given bound for the output voltage of inverters, which often leads to instability due to the integrator windup and undesired oscillations, see Paquette and Divan (2015); Konstantopoulos et al. (2016). Though a lot of anti-windup designs have been proposed, see Tarbouriech and Turner (2009), most of these methods need the complex designs. In this paper, a bounded-voltage power flow control with the bounded-voltage design based on the existing UDE-based robust power flow control in Wang et al. (2016a) is proposed for grid-tied PV systems, inspired by the bounded integral controller in Konstantopoulos et al. (2016). The boundedness analysis is provided via the Lyapunov method. With the introduction of bounded-voltage design, the inverter voltage always keeps within the given range. Hence, it can provide voltage protection in some failure-modes, e.g. sensor errors or grid voltage fluctuation, and can easily achieve voltage regulation in a whole islanded microgrid within the proposed methods, and avoid the integrator windup which might be caused by saturation units. In some cases, the reactive power is needed to feed into the grid from PV systems, e.g. the reactive power compensation or harmonics mitigation, see Wu et al. (2005); Deo et al. (2015). The reactive power setting is usually from a high-level control, e.g. microgrid controller. The bounded-voltage power flow control can stabilize the inverter voltage in the presence of the inappropriate setting of reactive power, or even in the network intrusion by hackers. For the whole grid-tied PV system, apart from the bounded-voltage power flow control, a gradient-based extremum seeking method developed in Ariyur and Krstic (2003); Ghaffari et al. (2014) is also adopted in this paper to achieve the MPPT. The DC-bus voltage is regulated by a UDE-based DC-bus voltage controller developed in Ren et al. (2017).

The rest of this paper is organized as follows. Section 2 provides system description. In Section 3, the bounded-voltage power flow control is proposed for DC/AC converter in grid-tied PV systems. Effectiveness of the proposed approach is demonstrated through simulation studies in Section 4 and experimental validation in Section 5, before the concluding remarks are made in Section 6.

2. SYSTEM DESCRIPTION

Fig. 1 demonstrates a typical structure for a grid-tied PV system, which consists of a PV source, a DC/DC converter converting DC power of PV source into a constant voltage DC bus, and a three-phase DC/AC converter feeding DC power into the AC grid. A DC-bus capacitor C_{pv} is placed between the PV source and the DC/DC converter to smooth the output voltage of PV source. Another DC-bus capacitor C_{dc} is placed between the DC/DC converter and the DC/AC converter to smooth the DC-bus voltage.

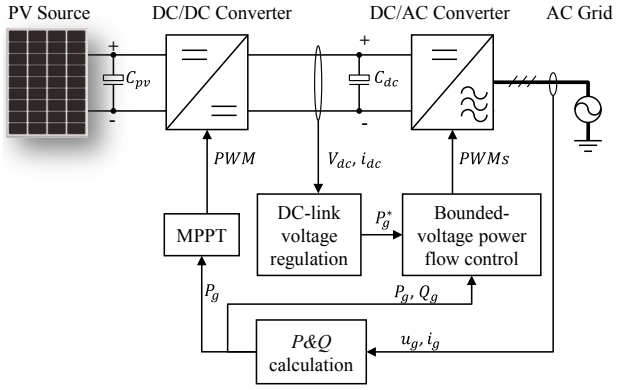

Fig. 1. System description of a PV system.

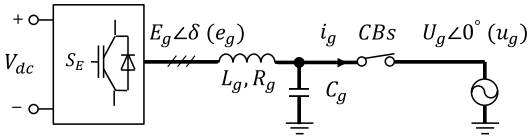

Fig. 2. DC/AC converter.

In this paper, the control strategy shown in Fig. 1, includes MPPT algorithm for the DC/DC converter, DC-bus voltage regulation and bounded-voltage power flow control for the DC/AC converter, and a power calculation unit to calculate real power P_g and reactive power Q_g based on both output voltage u_g and output current i_g of the DC/AC inverter. MPPT is used to maximize the real power output P_g. There is no need for the measurements of both output voltage and output current of the PV source. Through MPPT control with pulse-width modulation (PWM) signal, the DC/DC converter converts variable-voltage DC power of PV source into the DC-bus. The DC-bus voltage is stabilized at a constant level by the DC-bus voltage regulation unit. The bounded-voltage power flow control converts DC power from DC-bus to grid AC power with accurate power regulation.

This paper focuses on the design of bounded-voltage power flow control, while the detailed information about the design of MPPT, the UDE-based DC-bus voltage controller, and the UDE-based power flow control can be found in these three papers, see Ghaffari et al. (2014); Ren et al. (2017); Wang et al. (2016a). The MPPT algorithm is a gradient-based extremum seeking method, see Ariyur and Krstic (2003); Ghaffari et al. (2014), and the DC-bus voltage regulation is through a UDE-based DC-bus voltage controller developed in Ren et al. (2017). The bounded-voltage power flow control, will be discussed in Section 3, is an improved version of the UDE-based robust power flow control in Wang et al. (2016a), inspired by the bounded integral controller in Konstantopoulos et al. (2016).

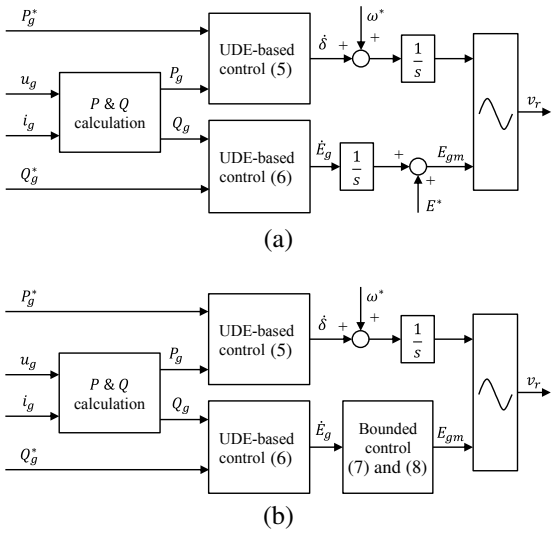

Fig. 3. The scheme of (a) the UDE-based robust power flow controller in Wang et al. (2016a), and (b) the proposed bounded-voltage power flow control.

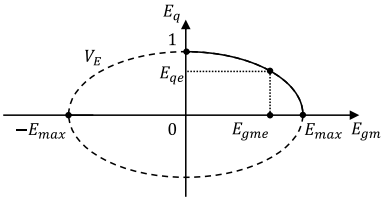

Fig. 4. Phase portrait of the voltage dynamics.

3. BOUNDED-VOLTAGE POWER FLOW CONTROL

3.1 Model of DC/AC converter

As shown in Fig. 2, the modeling of the DC/AC converter can be obtained as, see Zhong and Hornik (2013),

$$P_g = \left(\frac{E_g U_g}{Z_g}\cos\delta - \frac{U_g^2}{Z_g}\right)\cos\theta + \frac{E_g U_g}{Z_g}\sin\delta\sin\theta, \quad (1)$$

$$Q_g = \left(\frac{E_g U_g}{Z_g}\cos\delta - \frac{U_g^2}{Z_g}\right)\sin\theta - \frac{E_g U_g}{Z_g}\sin\delta\cos\theta, \quad (2)$$

where δ is the phase lead between the output voltage of inverter bridge $E_g\angle\delta$ and the grid $U_g\angle 0^\circ$, often called the power angle. The grid voltage u_g is used as the reference, so its initial angle is defined as zero. The output impedance Z_g is defined as $Z_g = R_g + X_g j$, where, the inductive impedance $X_g j$ is mostly dominated by L_g, as the output capacitor C_g is usually very small.

By taking derivatives of both (1) and (2), and following the procedures in Wang et al. (2016a), the dynamics of power delivering with both frequency dynamics and voltage dynamics can be obtained

$$\dot{P}_g = \frac{E_g U_g}{Z_g}\dot{\delta} + \triangle_p, \quad (3)$$

$$\dot{Q}_g = \frac{U_g}{Z_g}\dot{E}_g + \triangle_q, \quad (4)$$

where,

$$\triangle_p = \frac{E_g U_g \dot{\delta}}{Z_g}(\cos\delta\sin\theta - 1) - \frac{E_g U_g \dot{\delta}}{Z_g}\sin\delta\cos\theta + \frac{U_g \dot{E}_g}{Z_g}\cos\delta\cos\theta + \frac{U_g \dot{E}_g}{Z_g}\sin\delta\sin\theta,$$

$$\triangle_q = \frac{U_g \dot{E}_g}{Z_g}(\cos\delta\sin\theta - 1) - \frac{U_g \dot{E}_g}{Z_g}\sin\delta\sin\theta - \frac{E_g U_g \dot{\delta}}{Z_g}\cos\delta\cos\theta - \frac{U_g \dot{E}_g}{Z_g}\sin\delta\cos\theta,$$

represent the lumped uncertain terms, including the uncertainties, the nonlinearity, and the coupling effects of power angle δ and output impedance Z_g.

3.2 Controller Design

The UDE-based robust power flow controller proposed by Wang et al. (2016a), which is based on the dynamics of power delivering (3) and (4) and the procedures of UDE design in Zhong and Rees (2004) for robust control of grid-tied DC/AC inverters, is described by

$$\dot{\delta} = \frac{Z_g}{E_g U_g}\left[L^{-1}\left\{\frac{1}{1-G_{pf}(s)}\right\} * (\dot{P}_g^* + k_p e_p) - L^{-1}\left\{\frac{sG_{pf}(s)}{1-G_{pf}(s)}\right\} * P_g\right], \quad (5)$$

$$\dot{E}_g = \frac{Z_g}{U_g}\left[L^{-1}\left\{\frac{1}{1-G_{qf}(s)}\right\} * (\dot{Q}_g^* + k_q e_q) - L^{-1}\left\{\frac{sG_{qf}(s)}{1-G_{qf}(s)}\right\} * Q_g\right], \quad (6)$$

where P_g^* is the real power reference from the UDE-based DC-bus voltage regulation controller in Ren et al. (2017), as shown in Fig. 1, Q_g^* is the reactive power setting, which is usually equal to zero to provide a unity power factor, or can be set from a high-level controller; $e_p = P_g^* - P_g$, and $e_q = Q_g^* - Q_g$ are power tracking errors; $k_p > 0$ and $k_q > 0$ are the constant error feedback gains for the error dynamics equations

$$\dot{e}_p = -k_p e_p$$

and

$$\dot{e}_q = -k_q e_q.$$

The UDE filters $G_{pf}(s)$ and $G_{qf}(s)$ are strictly-proper stable filters with the appropriate bandwidth for the estimation of the uncertain terms $\triangle_p$ in (3) and $\triangle_q$ (4). Though the robustness of the UDE-based robust power flow controller is achieved in Wang et al. (2016a) to deal with the model uncertainties and the external disturbances with a simple structure, the bounded-voltage of the inverter with the voltage protection still has not been considered yet.

Here, a bounded-voltage power flow control is redesigned to maintain the given range for the inverter voltage, with the maximum value as E_{max}. Following the concept of bounded integral controller in Konstantopoulos et al. (2016), the voltage regulation (6) is modified with adding a bounded-voltage controller

Table 1. The parameters of the PV system for simulation studies.

Parameters	Values	Parameters	Values
L_g	2.2 mH	C_{dc}	1000 μF
R_g	0.5 Ω	DC-bus voltage	400 V
C_g	10 μF	Phase voltage $U_g/\sqrt{3}$	110 V_{rms}
C_{pv}	680 μF	Grid frequency	60 Hz

Table 2. Control parameters.

Parameters	Values	Parameters	Values
k_p	20	τ_p, τ_q	0.005 s
k_q	20	$E^*/\sqrt{3}$	110 V_{rms}
$G_{pf}(s)$	$\frac{1}{1+\tau_p s}$	k	1000
$G_{qf}(s)$	$\frac{1}{1+\tau_q s}$	E_{max}	$1.2E^*$

$$\dot{E}_{gm} = -k\left(\frac{E_{gm}^2}{E_{max}^2} + E_q^2 - 1\right)E_{gm} + E_q^2\dot{E}_g, \quad (7)$$

$$\dot{E}_q = -k\left(\frac{E_{gm}^2}{E_{max}^2} + E_q^2 - 1\right)E_q - \frac{E_q E_{gm}}{E_{max}^2}\dot{E}_g, \quad (8)$$

where E_{gm} is the modified voltage regulation output and E_q is an additional variable with the initial states $E_{gm0} = E^*$, $E_{q0} = \sqrt{1 - \frac{(E^*)^2}{E_{max}^2}}$, $E^*$is the nominal grid voltage, and $k > 0$ is a positive constant gain. The comparison between the original UDE-based robust power flow controller in Wang et al. (2016a) and the proposed bounded-voltage power flow controller is shown in Fig. 3.

Considering the following Lyapunov function candidate

$$V_E(t) = \frac{E_{gm}^2}{E_{max}^2} + E_q^2.$$

Taking the derivative of $V_E(t)$ along with (7) and (8) leads to

$$\begin{aligned}\dot{V}_E(t) &= \frac{2E_{gm}}{E_{max}^2}\dot{E}_{gm} + 2E_q\dot{E}_q \\ &= -\frac{2kE_{gm}}{E_{max}^2}\left(\frac{E_{gm}^2}{E_{max}^2} + E_q^2 - 1\right) + \frac{2E_{gm}}{E_{max}^2}E_q^2\dot{E}_g \\ &\quad -2kE_q^2\left(\frac{E_{gm}^2}{E_{max}^2} + E_q^2 - 1\right) - \frac{2E_q^2E_{gm}}{E_{max}^2}\dot{E}_g \\ &= -2k\left(\frac{E_{gm}^2}{E_{max}^2} + E_q^2\right)^2 + 2k\left(\frac{E_{gm}^2}{E_{max}^2} + E_q^2\right) \\ &= -2kV_E^2(t) + 2kV_E(t). \end{aligned} \quad (9)$$

Then, solving (9) gives

$$V_E(t) = \frac{e^{2kt}V_E(0)}{e^{2kt}V_E(0) - V_E(0) + 1}. \quad (10)$$

Given the initial conditions $E_{gm0} = E^*$, $E_{q0} = \sqrt{1 - \frac{(E^*)^2}{E_{max}^2}}$, there is

$$V_E(0) = 1 \Rightarrow V_E(t) = 1, \forall t \geq 0.$$

So,

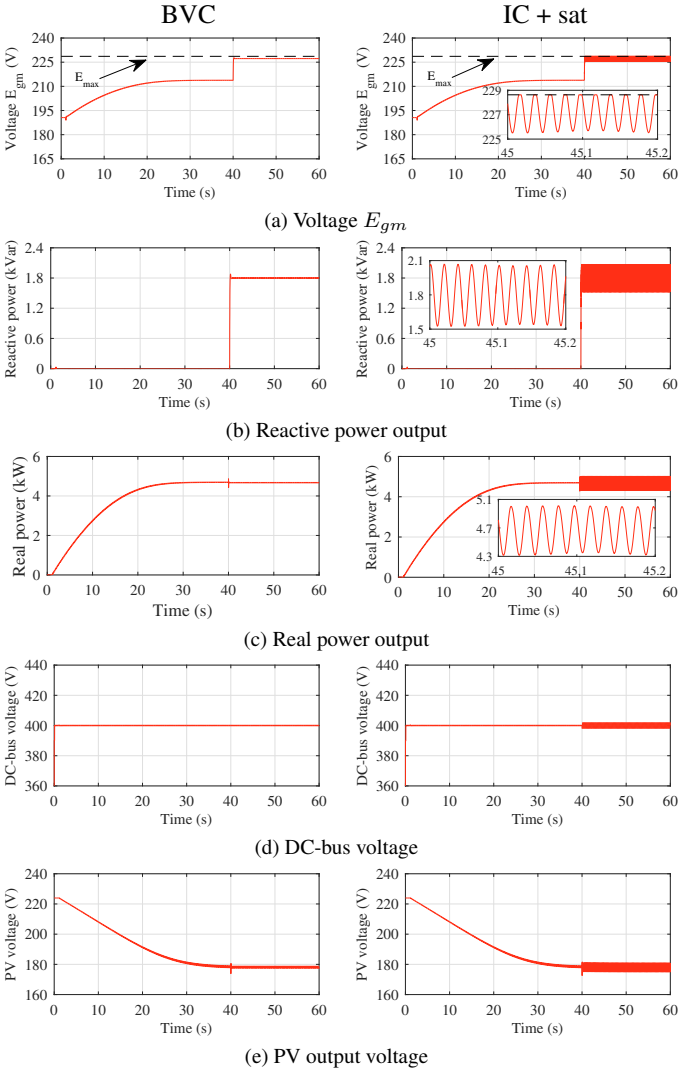

Fig. 5. Simulation results of PV system with BVC (left) and IC + saturation unit (right)

$$\frac{E_{gm}^2}{E_{max}^2} + E_q^2 = 1,$$

therefore, E_{gm} is always bounded in the given range $E_{gm} \in \{-E_{max} \leq E_{gm} \leq E_{max}\}$, and $E_q \in \{0 \leq E_q \leq 1\}$, no matter how $\dot{E}_g$ changes, as shown in Fig. 4. In a nominal condition, E_{gm} is greater than zero. In the steady-state, $\dot{E}_g$ needs to be regulated to 0. When $\dot{E}_g = 0$, both controller states E_{gm} and E_q will converge to the equilibrium point (E_{gme}, E_{qe}) as shown in Fig. 4.

4. SIMULATION STUDIES

To verify the effectiveness of the proposed bounded-voltage power flow control for grid-tied PV systems, a simulation platform with the same structure as Fig. 1 is built in MATLAB/Simulink/SimPowerSystems. The PV source is considered as 100 solar panels, RENOGY RNG-50P, see Wang et al. (2017), with a 10×10 series-parallels array. The DC/DC converter is a boost converter, and the grid is a three-phase AC grid. The detailed system parameters are listed in Table 1. The

Table 3. The parameters of the PV system for experimental validation.

Parameters	Values	Parameters	Values
L_g	200 μH	Grid voltage	20 V_{rms}
R_g	0.4 Ω	Grid frequency	60 Hz
C_g	3 μF	E^*	20 V_{rms}
DC-bus voltage	35 V	E_{max}	$1.1E^*$

parameters for bounded-voltage power flow control are provided in Table 2. Its performance is compared with the existing UDE-based robust power flow control developed in Wang et al. (2016a) by adding a saturation unit.

The system starts at $t = 0$ s. The sunlight is considered as 1000 W/m^2, and a very small duty cycle is set for DC/DC converter. The DC-bus voltage regulation starts when V_{dc} reaches 400 V, then the DC/AC converter delivers a small amount of power to the AC grid. The MPPT is enabled after $t = 1$ s. At $t = 40$ s, the reactive power is set as $Q_g^* = 1.8$ kVar. The system stops at $t = 60$ s.

Two controllers are studied in this simulation, the proposed bounded-voltage power flow control (BVC), and the existing UDE-based robust power flow control with a saturation unit (IC + sat). The system responses are shown in Fig. 5, including inverter voltage E_{gm} in Fig. 5(a), reactive power output in Fig. 5(b), and real power output in Fig. 5(c). After enabling MPPT, the real power output goes up to the maximum value within 25 s, the voltage E_{gm} goes up accordingly with the similar performances of two controllers, and the reactive power output keeps 0 Var. At $t = 40$ s, the reactive power reference is set as $Q_g^* = 1.8$ kVar, while the reactive power with BVC delivered to the grid keeps at a constant value, about 1.8 kVar, and the voltage E_{gm} almost reaches its maximum value E_{max} as shown in Fig. 5(a). The real power still keeps at the maximum value without oscillations. However, the IC with saturation results in a large transient with the integrator windup in the voltage E_{gm}, when the voltage E_{gm} is close to its maximum value E_{max} with the inappropriate setting of reactive power reference, as shown Fig. 5(a). Both real power and reactive power suffer from the big oscillations. The corresponding DC-bus voltage is shown in Fig. 5(d), and PV output voltage in Fig. 5(e). The oscillations on AC side by IC with saturation also affect the DC-bus voltage and PV output voltage. Therefore, the bounded-voltage power flow control can regulate the voltage E_{gm} within the specific range even in the presence of the inappropriate setting of reactive power reference, and avoid the integrator windup caused by the saturation unit.

5. EXPERIMENTAL VALIDATION

To further verify the proposed bounded-voltage power flow control for grid-tied PV systems, a test rig with one PV system (including a solar panel, RENOGY RNG-50P, and a Texas Instruments solar explorer kit embedded with DC/DC converter and the DC/AC converter) delivering power to a grid simulator is built for testing. The detailed system setup can be found in Wang et al. (2017). The system parameters are shown in Table 3, and control parameters are same as Table 2.

Initially, the system already operates at MPPT condition with a constant floodlight. At $t = 2$ s, the reactive power reference is set with $Q_{set} = 40$ Var. At $t = 5$ s, the grid voltage is changed from 20 V_{rms} to 21.5 V_{rms}.

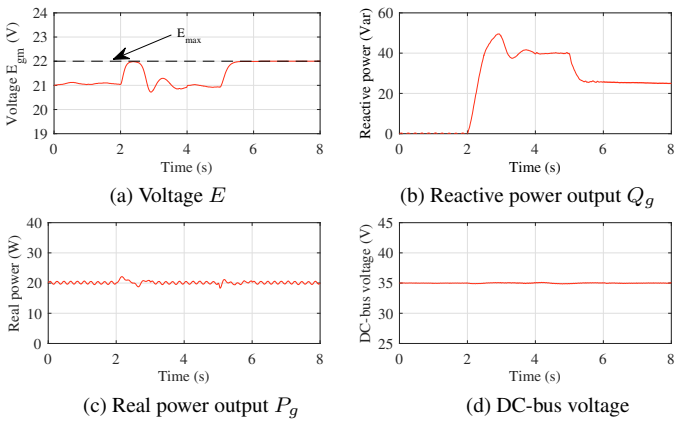

(a) Voltage E (b) Reactive power output Q_g

(c) Real power output P_g (d) DC-bus voltage

Fig. 6. Experimental results for safety protection

The system responses are shown in Fig. 6. The real power output is about 20 W in a constant floodlight with MPPT. After the reactive power is set to 40 Var, the proposed method regulates the output voltage E_{gm} inside the given bounded range within E_{max} of 22 V_{rms}, as shown in Fig. 6(a). Though the reactive power has some overshoots, it settles down quickly, as shown in Fig. 6(b). After $t = 5$ s, the grid voltage is changed to 21.5 V_{rms}, the reactive power drops to 25 Var within 0.5 s, as the voltage E_{gm} reaches its maximum value E_{max} as shown in Fig. 6(a). The real power keeps almost unchanged with only small spikes in the whole experimental period. The DC-bus voltage keeps steady well. Hence, the proposed bounded-voltage control can provide AC voltage protection by regulating the voltage E_{gm} within the specific range.

6. CONCLUSION

In this paper, a bounded-voltage power flow control has been proposed for grid-tied PV systems by integrating the bounded control into the existing UDE-based robust power flow control without the need of the saturation unit. With the bounded-voltage design, the voltage of the DC/AC converter always stays within the given range, which can avoid the integrator windup caused by the saturation unit and provide voltage protection facing the inappropriate setting of reactive power reference. The effectiveness of the proposed bounded-voltage power flow control has been validated by both simulation and experimental studies.

ACKNOWLEDGMENT

The authors would like to thank Texas Instruments for the donation of the inverter kits TIDM-HV-1PH-DCAC.

REFERENCES

Ariyur, K.B. and Krstic, M. (2003). *Real-Time Optimization by Extremum-Seeking Control*. Wiley-InterScience.

Beck, H.P. and Hesse, R. (2007). Virtual synchronous machine. In *Proc. of the 9th International Conference on Electrical Power Quality and Utilisation (EPQU)*, 1–6.

Deo, S., Jain, C., and Singh, B. (2015). A PLL-less scheme for single-phase grid interfaced load compensating solar PV generation system. *IEEE Trans. Ind. Informat.*, 11(3), 692–699.

Femia, N., Lisi, G., Petrone, G., Spagnuolo, G., and Vitelli, M. (2008). Distributed maximum power point tracking of photovoltaic arrays: Novel approach and system analysis. *IEEE Trans. Ind. Electron.*, 55(7), 2610–2621.

Femia, N., Petrone, G., Spagnuolo, G., and Vitelli, M. (2005). Optimization of perturb and observe maximum power point tracking method. *IEEE Trans. Power Electron.*, 20(4), 963–973.

Ghaffari, A., Krstic, M., and Seshagiri, S. (2014). Power optimization for photovoltaic microconverters using multivariable newton-based extremum seeking. *IEEE Trans. Control Syst. Technol.*, 22(6), 2141–2149.

Hua, C., Lin, J., and Shen, C. (1998). Implementation of a DSP-controlled photovoltaic system with peak power tracking. *IEEE Trans. Ind. Electron.*, 45(1), 99–107.

Killi, M. and Samanta, S. (2015). An adaptive voltage-sensor-based MPPT for photovoltaic systems with SEPIC converter including steady-state and drift analysis. *IEEE Trans. Ind. Electron.*, 62(12), 7609–7619.

Kim, J., Guerrero, J.M., Rodriguez, P., Teodorescu, R., and Nam, K. (2011). Mode adaptive droop control with virtual output impedances for an inverter-based flexible AC microgrid. *IEEE Trans. Power Electron.*, 26(3), 689–701.

Konstantopoulos, G.C., Zhong, Q.C., Ren, B., and Krstic, M. (2016). Bounded integral control of input-to-state practically stable non-linear systems to guarantee closed-loop stability. *IEEE Trans. Autom. Control*. DOI 10.1109/TAC.2016.2552978.

Koutroulis, E., Kalaitzakis, K., and Voulgaris, N.C. (2001). Development of a microcontroller-based, photovoltaic maximum power point tracking control system. *IEEE Trans. Power Electron.*, 16(1), 46–54.

Liu, W., Wang, K., Chung, H., and Chuang, S. (2015). Modeling and design of series voltage compensator for reduction of DC-link capacitance in grid-tie solar inverter. *IEEE Trans. Power Electron.*, 30(5), 2534–2548.

Montoya, D.G., Ramos-Paja, C.A., and Giral, R. (2016). Improved design of sliding-mode controllers based on the requirements of MPPT techniques. *IEEE Trans. Power Electron.*, 31(1), 235–247. doi:10.1109/TPEL.2015.2397831.

Nejabatkhah, F. and Li, Y.W. (2015). Overview of power management strategies of hybrid AC/DC microgrid. *IEEE Trans. Power Electron.*, 30(12), 7072–7089.

Paquette, A.D. and Divan, D.M. (2015). Virtual impedance current limiting for inverters in microgrids with synchronous generators. *IEEE Trans. Ind. Appl.*, 51(2), 1630–1638. doi: 10.1109/TIA.2014.2345877.

Pilawa-Podgurski, R.C.N. and Perreault, D.J. (2013). Submodule integrated distributed maximum power point tracking for solar photovoltaic applications. *IEEE Trans. Power Electron.*, 28(6), 2957–2967.

Prodanovic, M. and Green, T.C. (2003). Control and filter design of three-phase inverters for high power quality grid connection. *IEEE Trans. Power Electron.*, 18(1), 373–380.

Ren, B., Wang, Y., and Zhong, Q.C. (2017). UDE-based control of variable-speed wind turbine systems. *International Journal of Control*, 90(1), 121–136.

Roman, E., Alonso, R., Ibanez, P., Elorduizapatarietxe, S., and Goitia, D. (2006). Intelligent PV module for grid-connected PV systems. *IEEE Trans. Ind. Electron.*, 53(4), 1066–1073.

Tarbouriech, S. and Turner, M. (2009). Anti-windup design: an overview of some recent advances and open problems. *IET Contr. Theory Appl.*, 3(1), 1–19.

Teng, J.H., Huang, W.H., Hsu, T.A., and Wang, C.Y. (2016). Novel and fast maximum power point tracking for photovoltaic generation. *IEEE Trans. Ind. Electron.*, 63(8), 4955–4966.

Tey, K.S. and Mekhilef, S. (2014). Modified incremental conductance algorithm for photovoltaic system under partial shading conditions and load variation. 61(10), 5384–5392.

Trinh, Q.N. and Lee, H.H. (2014). An enhanced grid current compensator for grid-connected distributed generation under nonlinear loads and grid voltage distortions. *IEEE Trans. Ind. Electron.*, 61(12), 6528–6537.

Walker, G.R. and Sernia, P.C. (2004). Cascaded DC-DC converter connection of photovoltaic modules. *IEEE Trans. Power Electron.*, 19(4), 1130–1139.

Wang, Y., Ren, B., and Zhong, Q.C. (2016a). Robust power flow control of grid-connected inverters. *IEEE Trans. Ind. Electron.*, 63(11), 6887–6897.

Wang, Y., Ren, B., and Zhong, Q.C. (2016b). Robust power flow control of grid-tied inverters based on the uncertainty and disturbance estimator. In *Proc. American Control Conference*, 7450–7455.

Wang, Y., Ren, B., and Zhong, Q.C. (2017). Robust control of dc-dc boost converters for solar systems. In *Proc. American Control Conference*. To be published.

Wu, T.F., Nien, H.S., Shen, C.L., and Chen, T.M. (2005). A single-phase inverter system for PV power injection and active power filtering with nonlinear inductor consideration. *IEEE Trans. Ind. Appl.*, 41(4), 1075–1083.

Zhong, Q.C. (2016). Virtual synchronous machines: A unified interface for smart grid integration. *IEEE Power Electronics Magazine*, 3(4), 1–12.

Zhong, Q.C. and Hornik, T. (2013). *Control of Power Inverters in Renewable Energy and Smart Grid Integration*. Wiley-IEEE Press.

Zhong, Q.C., Konstantopoulos, G.C., Ren, B., and Krstic, M. (2016). Improved synchronverters with bounded frequency and voltage for smart grid integration. *IEEE Trans. Smart Grid*. DOI 10.1109/TSG.2016.2565663.

Zhong, Q.C. and Rees, D. (2004). Control of uncertain LTI systems based on an uncertainty and disturbance estimator. *Journal of Dyn. Sys. Meas. Con.Trans. ASME*, 126(4), 905–910.

Zhong, Q.C., Wang, Y., and Ren, B. (2017). UDE-based robust droop control of inverters in parallel operation. *IEEE Trans. Ind. Electron.* To be published, DOI 10.1109/TIE.2017.2677309.

Zhong, Q.C. and Weiss, G. (2009). Static synchronous generators for distributed generation and renewable energy. In *Proc. of IEEE PES Power Systems Conference & Exhibition (PSCE)*.

Zhong, Q.C. and Weiss, G. (2011). Synchronverters: Inverters that mimic synchronous generators. *IEEE Trans. Ind. Electron.*, 58(4), 1259–1267.